

Retrieval of middle-infrared reflectance using remote sensing data: the tropical point of view

Renata Libonati ^{1,3}
Carlos do Carmo de Portugal e Castro da Camara ¹
José Miguel Cardoso Pereira ²
Alberto W. Setzer ³
Leonardo de Faria Peres ³

¹Instituto Dom Luiz - IDL/CGUL
Campo Grande, Ed. C8 - Lisboa - Portugal
{rlsantos, cdcamara}@fc.ul.pt

²Instituto Superior de Agronomia - ISA/DF
Tapada da Ajuda- Lisboa - Portugal
jmocpereira@gmail.com

³Instituto Nacional de Pesquisas Espaciais - INPE
CEP 12630-000 – Cachoeira Paulista - SP, Brasil
{alberto.setzer, leonardo.peres}@cptec.inpe.br

Abstract. This work focuses on the problem of retrieving Middle infrared (MIR) surface reflectance from remote sensing information. The emphasis is on burned area discrimination and special attention is devoted to the method proposed by Kaufman and Remer in 1994 when applied in tropical environments. The analysis is based on simulated radiances for different conditions using MODTRAN-4. The best results regarding the ability of the method to distinguish between burned and unburned surfaces were obtained in the case of temperate conditions. In the case of tropical conditions the method has proven to be highly ineffective in distinguishing between the two classes since the estimated reflectance for vegetated surface may erroneously lead to identifying vegetation as a burned surface. This feature may therefore severely impair using Kaufman and Remer's method for burnt area discrimination over tropical regions such as Amazonia.

Palavras-chave: middle-infrared, burnt area, remote sensing, reflectance retrieval

1. Introduction

Current methods for detecting burned areas have mainly relied on information in the red (R) and near infrared (NIR) regions of the electromagnetic spectrum. However, both channels are very sensitive to aerosol scattering and absorption in the atmosphere (Fraser & Kaufman (1985), França & Setzer (1998)) and therefore traditional use of R and NIR channels for detecting burned areas over the Amazon region is severely impaired by the presence of heavy smoke layers due to biomass burning, since. A possible way to mitigate the aerosol effects associated to biomass burning is by using the middle-infrared (MIR) part of the spectrum (around 3.9 μm), since it is also sensitive to vegetation changes but is virtually unaffected by the presence of most aerosols. Several studies have shown that the use of MIR reflectance for the study of vegetation is promising for the discrimination of different vegetation types (Holben and Shimabukuro 1993, Shimabukuro et al. 1994, Goita et al. 1997); in particular, the work of Pereira (1999) indicated that spectral vegetation indices that use the R and NIR channels provide improved burned/unburned area discrimination when the R channel is replaced by the reflected component of the MIR channel. Although the use of reflected component of the MIR radiation appears to be very attractive, it presents several challenging problems linked to the diversity of radiance sources in a single measurement, namely the thermal emission and the solar reflection from the atmosphere and the surface. Existing

techniques for the MIR reflectance retrieval are time consuming and normally requires auxiliary datasets (e.g. atmospheric profiles) and large computational means (e.g. for radiative transfer computations). This is the case of the procedures proposed by e.g. Li & Becker (1993), Nerry et al. (1998) and Petitcolin & Vermote (2002) that, although providing the retrieval of MIR reflectance with acceptable accuracy, require huge auxiliary datasets and heavy numerical computations. A simple method was proposed by Kaufman and Remer (1994) where different assumptions are made to separate the thermal and solar components of the MIR signal. This method does not require heavy numerical computations and presents the major advantage of avoiding the use of auxiliary datasets. It was first designed to identify dense, dark vegetation areas in mid-latitude environments and has been widely used in burned area discrimination. Pereira (1999) has used the above mentioned approach in a study to assess the ability of several vegetation indices to discriminate between burned and unburned surfaces in Portugal. Barbosa et al., 1999 and Roy et al., 1999 have conducted a study over Africa where the reflective part of AVHRR channel 3 was extracted by using the methodology proposed by Kaufman & Remer (1994) in order to develop burned area algorithms.

Approximate solutions, like the one proposed by Kaufman & Remer (1994), are fast and easy to implement, but may not be accurate enough in specific conditions. Accordingly, the work presented in this article deals with the problem of retrieving the reflectance in the MIR spectral region with a particular emphasis on the accuracy achievable by means of Kaufman & Remer (1994) method in tropical environments. The next section provides an overview of the physical principles that governs the radiation in MIR spectral region together with a detailed review of the methodology proposed by Kaufman & Remer (1994).

2. Physics of the problem

The general expression for satellite measured radiance at the top of the atmosphere (TOA) level in the MIR channel for clear-sky conditions may be written in the form of an energy balance equation, which may be expressed as follows:

$$L_{\text{MIR}} = t_{\text{MIR}} \rho_{\text{MIR}} \frac{E_{0\text{MIR}}}{\pi} \mu_0 + \tau_{\text{MIR}} \varepsilon_{\text{MIR}} B(\lambda_{\text{MIR}}, T_s) + \tau_{\text{MIR}} \rho_{\text{MIR}} \bar{L}_{\text{atm, MIR}} \downarrow + L_{\text{atm, MIR}} \uparrow + L_s \quad (1)$$

where t_{MIR} is the two-way total atmospheric transmittance (sun-surface-sensor); ρ_{MIR} is the surface reflectance; $E_{0\text{MIR}}$ is the exo-atmospheric irradiance; μ_0 is the cosine of the solar zenith angle (SZA); τ_{MIR} is the one-way total atmospheric transmittance (surface-sensor); ε_{MIR} is the surface emissivity; $B(\lambda_{\text{MIR}}, T_s)$ is the emitted radiance given by Planck's function for the surface temperature T_s and the central wavelength λ_{MIR} ; $\bar{L}_{\text{atm, MIR}} \downarrow$ is the hemispherically averaged atmospheric downward thermal emission; $L_{\text{atm, MIR}} \uparrow$ is the atmospheric upward thermal emission and L_s is the term associated with atmospheric scattering. The first term on the right-hand side of (1) represents the solar radiance that is attenuated by the atmosphere in its downward path, reflected by the surface and again attenuated in its upward path to the sensor. The second term represents the radiance emitted by the surface that is attenuated by the atmosphere. The third term denotes the downward atmospheric radiance that is reflected by the surface and then attenuated in its upward path to the sensor. The fourth term represents the radiance emitted by the atmosphere towards the sensor. Finally, as previously mentioned, the last term is associated with atmospheric scattering.

Assuming the Earth's surface behaves as a Lambertian emitter-reflector, surface reflectance and emissivity are related as ($\rho_{\text{MIR}} = 1 - \varepsilon_{\text{MIR}}$). Neglecting the atmospheric scattering term, L_{S} , the solution of equation (1) is given by:

$$\rho_{\text{MIR}} = \frac{L_{\text{MIR}} - \tau_{\text{MIR}} B(\lambda_{\text{MIR}}, T_{\text{S}}) - L_{\text{atm,MIR}} \uparrow}{t_{\text{MIR}} \frac{E_{0\text{MIR}}}{\pi} \mu_0 - \tau_{\text{MIR}} B(\lambda_{\text{MIR}}, T_{\text{S}}) + \tau_{\text{MIR}} \bar{L}_{\text{atm,MIR}} \downarrow} \quad (2)$$

Problems encountered in estimating MIR reflectance based on the radiative transfer equation (RTE), Equation (2), originate from the diversity of radiance sources (e.g., thermal emission and solar reflection from atmosphere and surface) in a single measurement, the uncertainties in the land surface temperature, the atmospheric correction and angular effects. Consequently, the usefulness of methods that take into account the major constituents of the MIR signal depends on available auxiliary datasets (e.g. atmospheric profiles) as well on the computational requirements (e.g. radiative transfer computations). Simple methods, such the one proposed by Kaufman and Remer (1994), allow retrieving MIR reflectance without a direct knowledge of the atmospheric state and any radiative transfer model. This approach is based on the study of Gessel (1989), that pointed out a mutual compensation of attenuation and thermal emission terms, so that both atmospheric transmittances (i.e. t_{MIR} and τ_{MIR}) may be assumed to be equal to unity and both the atmospheric downward and upward thermal emission terms may be neglected. Considering the above mentioned assumptions, and using the brightness temperature from a thermal infrared (TIR) band ($T_{\text{B,TIR}}$) as a surrogate for T_{S} , leads to:

$$\rho_{\text{MIR}} = \frac{L_{\text{MIR}} - B(\lambda_{\text{MIR}}, T_{\text{B,TIR}})}{\frac{E_{0\text{MIR}}}{\pi} \mu_0 - B(\lambda_{\text{MIR}}, T_{\text{B,TIR}})} \quad (3)$$

The use of a temperature lower than T_{S} (such as $T_{\text{B,TIR}}$) tends to compensate the net effect resulting from the assumptions that the contributions from atmospheric emission are null and that the transmission functions are both equal to unity.

Equation (3) has been used in a number of environment studies in both temperate and tropical conditions (e.g. Barbosa et al., 1999; Boyd, 1999, Holben & Shimabukuro, 1993; Pereira, 1999). Although these studies show promising results, none of them have take into account a quantitative estimation of the error associated with the MIR reflectance retrieval from Equation (3) over tropical conditions. Accordingly, we have carried out a sensitivity analysis of the above mentioned methodology and its influence on the MIR reflectance retrieval under tropical environments.

3. Data

We have performed radiative transfer simulations using MODTRAN-4 radiative transfer model (Berk et al., 2000) for a wide variety of atmospheric, surface and geometry conditions. The simulations were spectrally performed in the range 3.62-3.97 μm and 10-12 μm (in steps of 1 cm^{-1}), and then the mean value and the root mean square deviation have been calculated. This option has been chosen instead of using a particular response function in order to obtain general results and not particularized for any sensor. The TIR region between 10 and 12 μm was used in order to calculate the brightness temperature needed as input of Equation (3), hereafter refereed to KFE.

The atmospheric contribution was computed for three geographical–seasonal model atmospheres stored in MODTRAN-4, namely Mid-Latitude Summer (MLS), Mid-Latitude Winter (MLW), and Tropical (TRO), that allow covering a wide range of atmospheric conditions, with water vapor content of 0.85, 2.92 and 4.11 g cm⁻² and 2m-air temperature (T_{atm}) of 272.2, 294.2 and 299.7 K, respectively. The assigned LST values were based on the 2-m air temperature, T_{atm} , of each profile, varying from T_{atm} to $T_{\text{atm}} + 30.0$ K in steps of 1.0 K, totalizing 31 different values. The sun–view geometry was characterized by three view zenith angles (VZA), i.e., 0°, 30° and 60°, and 31 solar zenith angles (SZA), from 0° to 60° in steps of 2°.

Surface emissivity values were based on information from charcoal and vegetation emissivity spectra (Figure 1). Charcoal data were provided by the NASA Jet Propulsion Laboratory with a Beckman UV5240 spectrophotometer, based on samples of fire residues of four different kind of tropical trees collected at Alta Floresta, state of Mato Grosso, Brazil. The dataset of vegetation emissivity was obtained from the MODIS-UCSB spectral library, including most vegetation types, with 25 surfaces emissivities varying from 0.96 to 0.99 in MIR channel. Finally we have prescribed a typical value of 0.24 (0.03) for charcoal (vegetation) MIR surface reflectance, which were obtained by averaging the MIR spectral signature of the four (25) considered charcoal (vegetation) surfaces. Accordingly, the synthetic data set are based on 3 atmospheres \times 31 values of land-surface temperature \times 3 viewing angles \times 31 values of solar zenith angles \times 2 surface reflectance = 17,298 simulations.

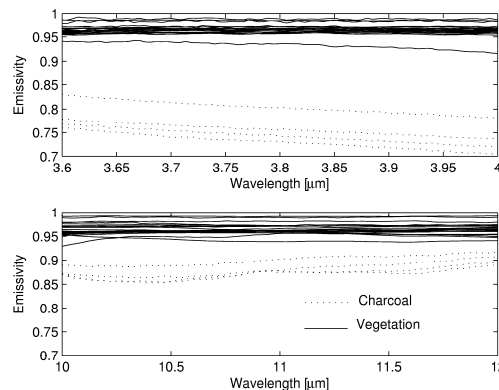


Figure. 1. Spectral signatures from four samples of charcoal (dot-curves) and from 25 samples of vegetation (solid curves). Charcoal and vegetation signatures were respectively obtained from samples of fire residues from Alta Floresta, state of Mato Grosso, Brazil and from the MODIS-UCSB spectral library.

4. Analysis and results

The KFE method is a simplified way that avoids having to take into consideration the atmospheric influence on remotely sensed retrieved MIR reflectance. The procedure thus relies on a number of assumptions concerning atmospheric transmittances and the atmospheric downward and upward thermal emission radiances. These parameters are correlated and depend essentially on the atmospheric water vapor content. Hence, when the atmospheric water vapor increases, the atmospheric transmittances decrease and the atmospheric downward and upward thermal emission radiances increase. Table 1 shows the values for the atmospheric parameters for the three considered profiles. Although the atmospheric parameters are correlated and depend on the water vapor, it may be interesting to analyze the effect of each parameter independently. For example, for a hot and wet atmosphere, such as TRO, the uncertainty of the assumption $\tau_{\text{MIR}} = 1$ ($t_{\text{MIR}} = 1$) is about

26.58% (53.80%) while for a MLW condition is only 9.90% (23.45%). As a result, the approximation used in KFE, namely atmospheric transmittances assumed to be equal to unity and both the atmospheric downward and upward thermal emission terms neglected, will have less impact in MLW than in TRO atmospheres. Results, therefore, obviously confirm that KFE may be less trustworthy at the tropics.

Table 1. Effects of water vapor content on the atmospheric parameters for the three considered profiles considering nadir view and a SZA of 0°.

Profile	τ_{MIR}	t_{MIR}	$L_{\text{atm,MIR}}^{\uparrow}$ [W m ⁻² μm ⁻¹ sr ⁻¹]	$\bar{L}_{\text{atm,MIR}}^{\downarrow}$ [W m ⁻² μm ⁻¹ sr ⁻¹]
TRO	0.79	0.65	0.057	0.104
MLS	0.83	0.70	0.038	0.068
MLW	0.91	0.81	0.006	0.012

The accuracy of the solutions to KFE was assessed by evaluating the retrieval errors, defined as the differences between retrieved values of MIR reflectance by means of (4) and the corresponding prescribed values as input to MODTRAN-4. Figures 2-4 show the relative error on retrieved MIR reflectance for nadir-viewing depending on the land surface temperature and solar zenith angle for charcoal and vegetation surfaces in the case of TRO, MLS and MLW profiles, respectively. It may be noted that the scales of LST are different for each profile, accordingly to real conditions and based on the 2-m air temperature of each profile stored in MODTRAN-4.

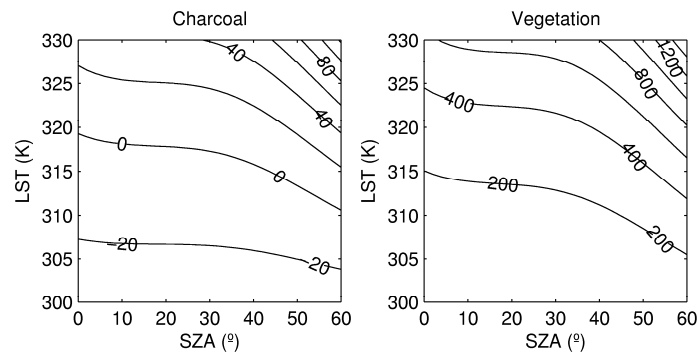


Figure 2. Relative error (%) on retrieved MIR reflectance for nadir-view depending on the land surface temperature and solar zenith angle in the case of TRO profile for charcoal (left) and vegetation (right).

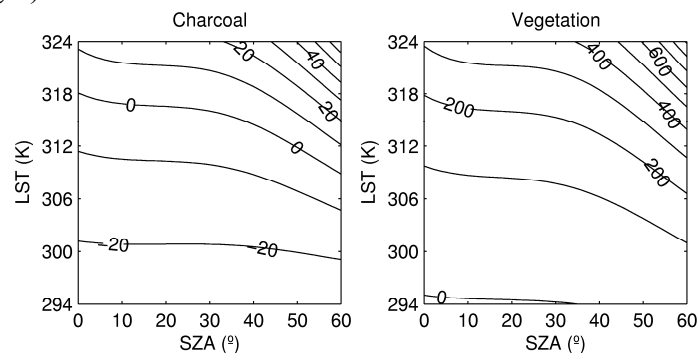


Figure 3. Same as Figure 1 but for MLS profile.

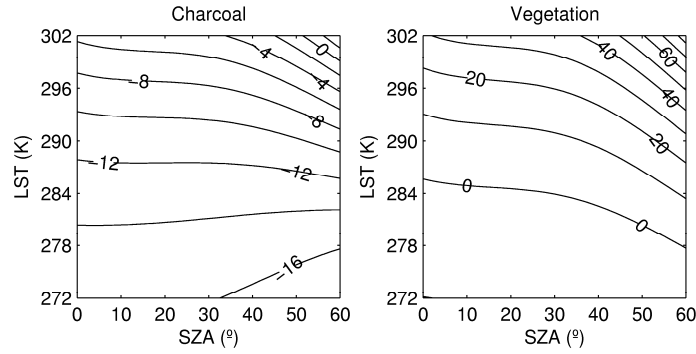


Figure 4. Same as Figure 1 but for MLW profile.

As expected the error values increase from a cold and dry atmosphere to a hot and wet one. It should be noted that the MLW values correspond well to those found Kaufman and Remer (1994) who estimated the accuracy of equation (5) to be around 0.01 and 0.02 for a mid-latitude atmosphere in the range of emissivities expected by a variety of vegetation and soils (0.94 – 1.00). In the range of temperatures expected for a TRO profile in the vegetation surface case, the uncertainty in the surface reflectance varies from 100% to 1200% from a true reflectance of 0.02, depending upon the LST and SZA. This correspond to absolute errors of 0.02 - 0.4. For the charcoal case, our results indicate relative errors of -20% to 80%, which correspond to absolute errors of - 0.05 – 0.2, depending upon the LST and SZA. The magnitude of the errors for vegetated surfaces shows that it becomes difficult to obtain accurate discrimination between unburned and burned surfaces at hot and wet atmospheres. For example, an error of 0.2 leads to a reflectance of 0.23 for vegetation, which is the same value of charcoal reflectance.

In order to demonstrate the disadvantages of using KFE algorithm at tropical conditions with the aim of discriminating between burned and unburned surfaces, we have generated a synthetic image in which each one of the retrieved values of MIR reflectance from our simulations is considered as a pixel of the image. The measure used to quantify the effectiveness to separate burned surfaces from the unburned background environment is given by:

$$M = \frac{|\mu_u - \mu_b|}{\sigma_u + \sigma_b} \quad (4)$$

where μ_u (μ_b) is the mean value for the unburned (burned) class and σ_u (σ_b) the standard deviation for the unburned (burned) class. Values of M larger than one indicate good separability, while values smaller than one represent a large degree of histogram overlap between the two classes. Table 2 presents the values of the M index and of the mean and standard deviation for the unburned (burned) class for each atmospheric profile. Figure 5 is a synthetic image showing: i) MIR surface reflectance of a real surface for burned (black) and unburned (green) surfaces; and MIR surface reflectance retrieved at ii) Tropical; iii) Mid-latitude summer and iv) Mid-latitude winter conditions. Results clearly show that KFE allows a better separation between burned and unburned surfaces in MLW, while in TRO there is a higher degree of overlap. In the case of MLW, the discrimination between the two classes is very clear, essentially due to the very small variance within and between-groups, since the means are widely separated and the standard deviations are small. In the case of TRO the method is not able to separate the means, and there is also a very large within-group variance. The MLS performs better TRO by exhibiting an intermediate behavior.

Table 2. M index and the mean and standard deviation values for the unburned (burned) class for each atmospheric profile.

	μ CHARCOAL	μ VEGETATION	σ CHARCOAL	σ VEGETATION	M
TRO	0.255	0.159	0.077	0.103	0.53
MLS	0.228	0.099	0.049	0.063	1.14
MLW	0.210	0.035	0.012	0.006	9.17

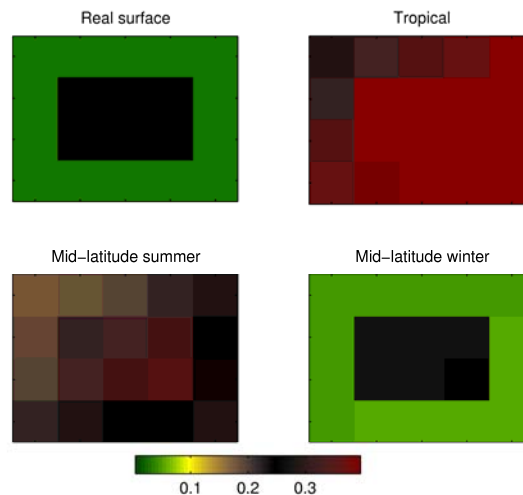


Figure 5. Synthetic image showing: i) MIR surface reflectance of a real surface (upper-left panel) for burned (black) and unburned (green) surfaces; and MIR surface reflectance retrieved at ii) Tropical (upper-right panel); iii) Mid-latitude summer (lower-left panel) and iv) Mid-latitude winter conditions (lower-right panel).

5. Conclusions

The major advantage of the methodology provided by Kaufman and Remer (1994) is to enable for a retrieval of MIR reflectance without the need for auxiliary datasets (e.g. atmospheric profiles) and major computational means (e.g. for radiative transfer computations). The method reveals to be especially adequate over areas where the atmosphere does not have significant influence on the radiance observed by satellites. This algorithm has been successfully used for burned area discrimination in mid-latitude regions (Pereira, 1999) but problems may arise when applying it in tropical environments. This is due to the fact that Kaufman and Remer's algorithm is based on the assumptions that the atmospheric contributions may be neglected and that atmospheric transmittance may be set to unity. Methods that allow recovering MIR reflectance without taking into account atmospheric information, may lead to undesirable results which strongly depend on atmospheric conditions. In the present case of burned area discrimination in tropical environments, the assumption of neglecting the atmospheric contributions and of setting the transmittance equal to unity will have an undesirable impact on the quality of results. In fact, KFE will be appropriate for cold and dry atmospheres and should be used with care in the case of hot and wet atmospheric conditions. Results show that, in the case of TRO, the prescribed hypotheses by Kaufman and Remer (1994) lead to errors of the same order of magnitude as the one of the reflectance to be estimated, reaching, in some cases, several order of magnitude higher than this value, especially for vegetated surfaces. In fact, KFE will be appropriate for cold and dry atmospheres and should be used with care in the case of hot and wet atmospheric conditions.

We have also performed a comparative study between the net effect of applying KFE in tropical and mid-latitudes conditions. The measure, M, used to quantify the effectiveness of the method is analogous to the signal-to-noise ratio concept. The largest ability to distinguish

between burned and unburned surfaces ($M = 9.17$) was obtained in MLW conditions. In the case of TRO the method has demonstrated to be ineffective to distinguish between the two classes ($M = 0.53$). These results may be viewed as validation approach of the KFE in different conditions.

In this way, the discrimination of burned areas using KFE in tropical environment is severely impaired, since the estimated reflectance for vegetated surface may be confused with burned area. These features may therefore severely impair the usage of Kaufman and Remer's algorithm for burnt area discrimination over tropical regions such as Amazonia.

ACKNOWLEDGMENTS

The Portuguese Foundation of Science and Technology (FCT) has supported the research performed by the first author (Grant No. SFRH/BD/21650/2005).

REFERENCES

- Barbosa, P.M., Gregoire, J.-M., and Pereira, J.M.C. An algorithm for extracting burned areas from time series of AVHRR GAC data applied at a continental scale. **Remote Sensing of Environment**, v. 69, p. 253–263, 1999.
- Berk, A., Anderson, G.P., Acharya, P.K., Chetwynd, J.H., Bernstein, L.S., Shettle, E.P., Matthew, M.W., & Alder-Golden, S.M. **MODTRAN4 version 2 user's manual**. Air Force Research Laboratory, Space Vehicles Directorate, Air Force Material Command, Hanscom AFB, MA 01731-3010, 2000.
- Boyd, D.S. The relationship between the biomass of Cameroonian tropical forests and radiation reflected in middle infrared wavelengths (3.0-5.0 μm). **International Journal of Remote Sensing**, v. 20, p. 1017-1023, 1999.
- Fraser, R.S., and Kaufman, Y.J. The relative importance of aerosol scattering and absorption in remote sensing. **IEEE Transactions on Geoscience and Remote Sensing**, v. 23, p. 525–633, 1985.
- Gesell, An algorithm for snow and ice detection using AVHRR data: An extension to the APOLLO software package. **International Journal of Remote Sensing**, v. 10, p. 897–905, 1989.
- Goita, K., and Royer, A. Surface temperature and emissivity separability over land surface from combined TIR and SWIR AVHRR data. **IEEE Transactions on Geoscience and Remote Sensing**, v. 35, p. 718–733, 1997.
- Holben, B.N., and Shimabukuro, Y.E. Linear mixing model applied to coarse spatial resolution data from multi-spectral satellite sensors. **International Journal of Remote Sensing**, v. 14, p. 2231–2240, 1993.
- Kaufman, Y. J., and Remer, L. Detection of forests using mid-IR reflectance: An application for aerosol studies. **IEEE Transactions on Geoscience and Remote Sensing**, v. 32(3), p. 672-683, 1994.
- Li, Z.-L., and Becker, F. Feasibility of land surface temperature and emissivity determination from NOAA/AVHRR data. **Remote Sensing of Environment**, v. 43, p. 1–20, 1993.
- Nerry, F., Petitcolin, F., and Stoll, M.-P. Bidirectional reflectivity in AVHRR channel 3: application to a region in northern Africa. **Remote Sensing of Environment**, v. 66, p. 298–316, 1998.
- Pereira, J.M.C. A comparative evaluation of NOAA/AVHRR vegetation indexes for burned surface detection and mapping. **IEEE Transactions on Geoscience and Remote Sensing**, v. 37(1), p. 217-226, 1999.
- Petitcolin, F., and Vermote, E. Land surface reflectance, emissivity and temperature from MODIS middle and thermal infrared data. **Remote Sensing of Environment**, v. 83, p. 112–134, 2002.
- Shimabukuro, Y. E., Holben, B. N., and Tucker, C. J. Fraction images derived from NOAA AVHRR data for studying the deforestation in the Brazilian Amazon. **International Journal of Remote Sensing**, v. 15, p. 517–520, 1994.